Supplementary Information

Janus structural TaO/TaN heterojunction as efficient oxygen reduction electrocatalyst for H_2O_2 production

Mei Li[▽], *Ting Yang*[▽], *Wenling Du, Jiaxin Bai, Haoran Ma, Jiansheng Liu and Zhanli Chai**

Inner Mongolia Key Laboratory of Rare Earth Catalysis, School of Chemistry and Chemical Engineering, Inner Mongolia University, Hohhot 010021, China

[▽]Mei Li and Ting Yang contributed equally to this work.

E-mail: chaizhanli@imu.edu.cn

Experimental Section

Materials

Tantalum(V) chloride (99.99%), n-butyl alcohol, Nafion 117 membrane, Nafion perfluorinated resin solution (5 wt.% in lower aliphatic alcohols and water, contains 15-20% water), KOH (90%), urea (99%), Toray carbon paper (TGP-H-060, wet proofed) were purchased from Fuel Cell Store.

Preparation of catalysts

1.0 g of $TaCl_5$ and 1.26 g urea (mole ratio of urea/$TaCl_5$ were 7.5) were added into 2.0 mL of n-butanol. The mixture was stirred for 1 h to obtain a colloidal substance, which was subsequently heated in a tubular furnace to 1000^{o}C with the rate of 2^{o}C/ min and maintained for 4 h. After cooling naturally, the precipitate was washed with ethanol and deionized water three times. The obtained product was denoted as TaO/TaN@Gr. Additionally, TaON@Gr composite was obtained by adjusting the mole ratio of urea/$TaCl_5$ to 10, which was denoted as TaON@Gr.

Characterizations

XRD patterns were acquired on a PANalytic Empyrean diffractometer with scan range of 5°-80°. SEM images were collected on a Regulus 8100 scanning electron microscope at an accelerating voltage of 10 kV. XPS measurements were performed on an Thermo ESCALAB250XI X-ray photoelectron spectrometer using Al as the exciting source. Raman spectroscopy measurements were performed on a DXRMicroscope Raman imaging microscope system with an excitation wavelength of 532 nm. TEM, HRTEM and STEM mapping images were collected on a FEI Tecnai G2 F20 SWIN transmission electron microscope operated at 200 kV, equipped with a high-angle annular dark-field detector (HADDF) and an energy dispersive spectrometer (EDS).

Electrochemical measurements

Rotating ring-disk electrode test: The catalytic ORR performance was evaluated in an O_2-saturated 0.1 M KOH solution by using a three-electrode system at an electrochemical workstation (CHI760E B19218). The Pt wire was used as the counter electrode, and the Ag/AgCl electrode was the reference electrode. A rotating ring-disk electrode (RRDE) was

used as the working electrode. The Pt ring electrode had an area of 0.1884 cm^2 , and the glass carbon disk electrode had an area of 0.1236 cm^2. The ring currents (I_{ring}) were collected by the Pt ring electrode, and the disk currents (I_{disk}) were measured by the glassy carbon disk electrode. The ring collection efficiency (N) was measured through a bare RRDE electrode in a 1 M KCl electrolyte with 10 mM $K_3[Fe(CN)_6]$. RRDE voltammograms were recorded at different rotation rates (400, 625, 900, 1225, 1600, 2025 rpm) by performing LSV curves, as shown in Fig. S7a. Accordingly, the ring collection efficiency was calculated as 0.37, as seen in Fig. S7b.

5.0 mg of catalyst were sonicated and dispersed into absolute alcohol (900 μL) containing 50 μL of 5 wt.% Nafion solutions. Then 5 μL inks were dropped onto the polished RRDE. All the measurements were carried out in O_2-saturated 0.10 M KOH solution. The rotating speed of RRDE was 1600 rpm. The ring electrode was set at a constant potential of 1.20 V vs. RHE (reversible hydrogen electrode) to detect the generated H_2O_2. All the recorded potentials were corrected to the RHE by calibration and all the electrocatalysts were stabilized in advance by cyclic voltammetry (CV) with a scan rate of 10 mV s^{-1}. And then linear sweep voltammetry (LSV) was conducted at a scan rate of 5 mV s^{-1}. The selectivity of H_2O_2 (the percentage of H_2O_2 in the product released during oxygen reduction reaction), the number of electrons transferred (n) and the Faradaic efficiency (FE %) were calculated from the disk current (I_{disk}) and ring current (I_{ring}) based on the following equation (1), (2) and (3), respectively.

$$H_2O_2\% = \frac{200 \times I_{ring}}{N \times |I_{disk}| + I_{ring}} \tag{1}$$

$$n = \frac{4|I_{disk}|}{|I_{disk}| + \frac{I_{ring}}{N}} \tag{2}$$

$$FE\% = \frac{|I_{ring}|/N}{|I_{disk}|} \times 100\% \tag{3}$$

And Tafel slopes were calculated from the Tafel equation (4):

$$\eta = b \times log\ (j/j_0) \tag{4}$$

Where η is the overpotential, b is the Tafel slope, j is the current density, and j_0 is the exchange current density.

Electrolysis in H-type cell: The measurement of H_2O_2 production was measured using a three-electrode H-type cell. A Pt wire electrode and Ag|AgCl (saturated KCl) electrode were employed as the counter and reference electrodes, respectively. The carbon paper (1cm×1cm) was used as the working electrode with the TaO/TaN@Gr catalyst loading of 0.2 mg. The electrolyte is 50 mL of 0.1 mol/L KOH solution. In the process of a H-type cell for H_2O_2 yield test, the rate of O_2 flow was controlled at 10 mL/min, while the potential was set at a fixed value (0.1, 0.2, 0.3, 0.4, 0.5, 0.6, 0.7 and 0.8 V), the catalyst was subjected to a 1h chronoamperometric (i-t) test combined with UV-visible spectroscopy to calculate the H_2O_2 yield.

The H_2O_2 concentration was quantified through a Ce^{4+} titration method. And the Ce^{4+} concentration was determined using UV-vis spectrophotometer. For known concentrations of 0.2, 0.3, 0.4, 0.5 and 0.6 mM of Ce^{4+}, the calibration curve was plotted by linearly fitting the absorbance values at a wavelength length of 319 nm (Fig. S8). The obtained aliquots of electrolyte after test were mixed with 1 mL 1 mM Ce^{4+} solution, and the absorbance at 319 nm was then measured by the spectrophotometer. The yield of H_2O_2 could be calculated from the reduced Ce^{4+} concentration.

DFT calculations

The Vienna Ab Initio Package (VASP) was employed to perform all the density functional theory (DFT) calculations within the generalized gradient approximation (GGA) using the Perdew, Burke, and Enzerhof (PBE) formulation. The projected augmented wave (PAW) potentials were applied to describe the ionic cores and take valence electrons into account using a plane wave basis set with a kinetic energy cutoff of 450 eV. Partial occupancies of the Kohn–Sham orbitals were allowed using the Gaussian smearing method and a width of 0.05 eV. The electronic energy was considered self-consistent when the energy change was smaller than 10^{-5} eV. A geometry optimization was considered convergent when the force change was smaller than 0.05 eV/Å. Grimme's DFT-D3 methodology was used to describe the dispersion interactions. The vacuum spacing perpendicular to the plane of the structure is 20 Å. The

Brillouin zone integral utilized the surfaces structures of 2×2×1 monkhorst pack K-point sampling. The charge density difference of system was determined by the function (5):

$$\Delta\rho = \rho_{total} - \rho_A - \rho_B \quad (5)$$

where ρ_{total} is the charge density of Binding systems, ρ_A and ρ_B is the sub charge density. Finally, the adsorption energies(E_{ads}) were calculated as following equation (6):

$$E_{ads} = E_{ad/sub} - E_{ad} - E_{sub} \quad (6)$$

where $E_{ad/sub}$, E_{ad}, and E_{sub} are the total energies of the optimized adsorbate/substrate system, the adsorbate in the structure, and the clean substrate, respectively. The free energy was calculated using the equation (7):

$$G=E_{ads}+ZPE-TS \quad (7)$$

where G, E_{ads}, ZPE and TS are the free energy, total energy from DFT calculations, zero point energy and entropic contributions, respectively.

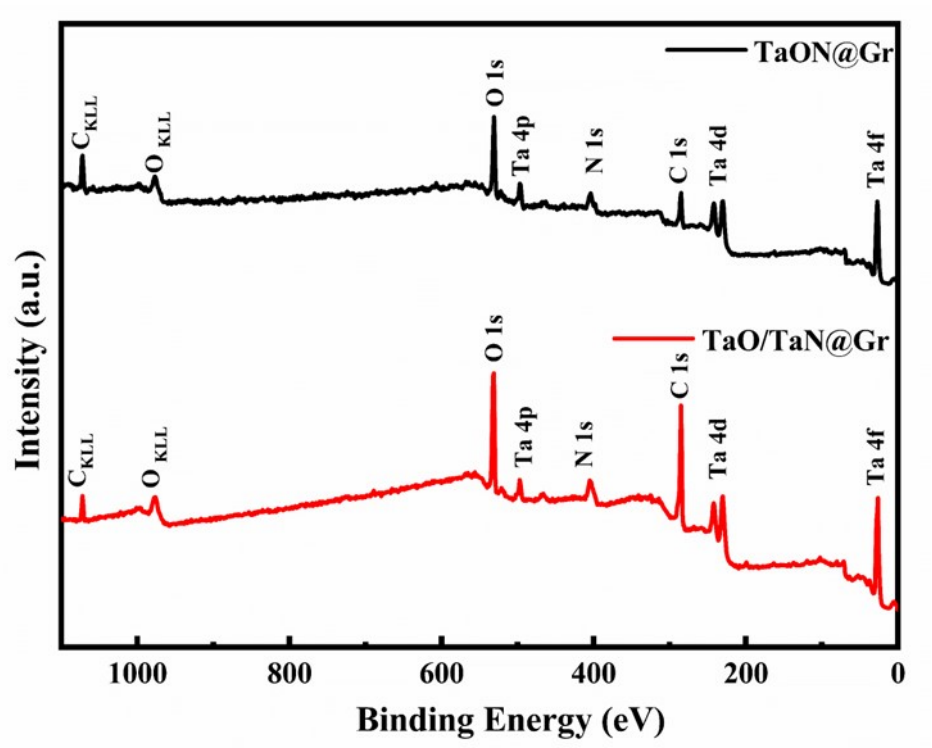

Fig. S1 The survey spectra of (a) TaON@Gr and (b) TaO/TaN@Gr.

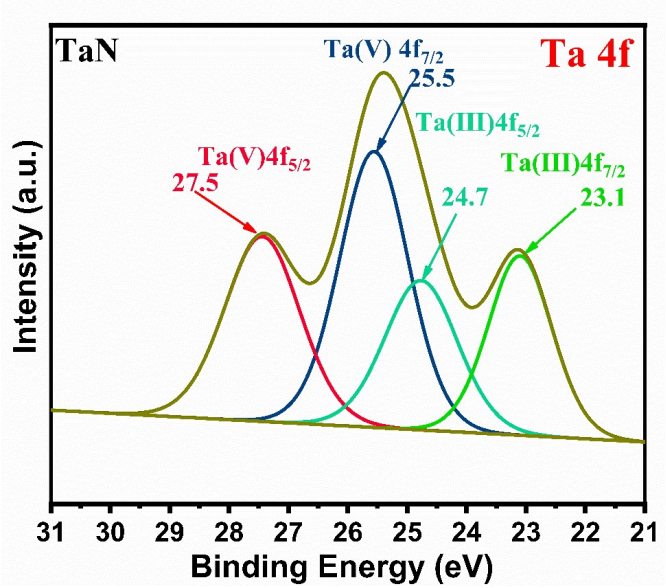

Fig. S2 XPS spectra of commercial TaN.

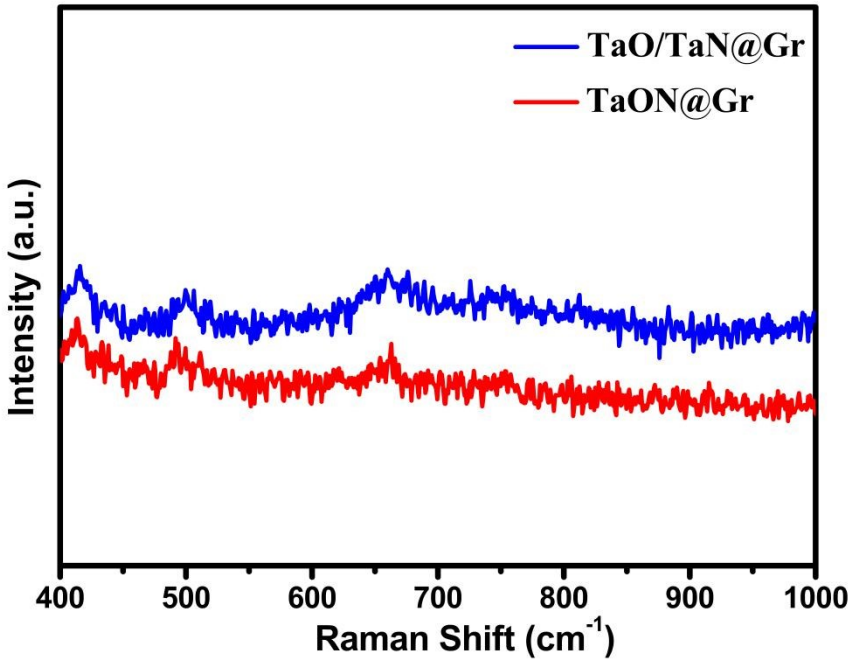

Fig. S3 Raman spectra of TaON@Gr and TaO/TaN@Gr.

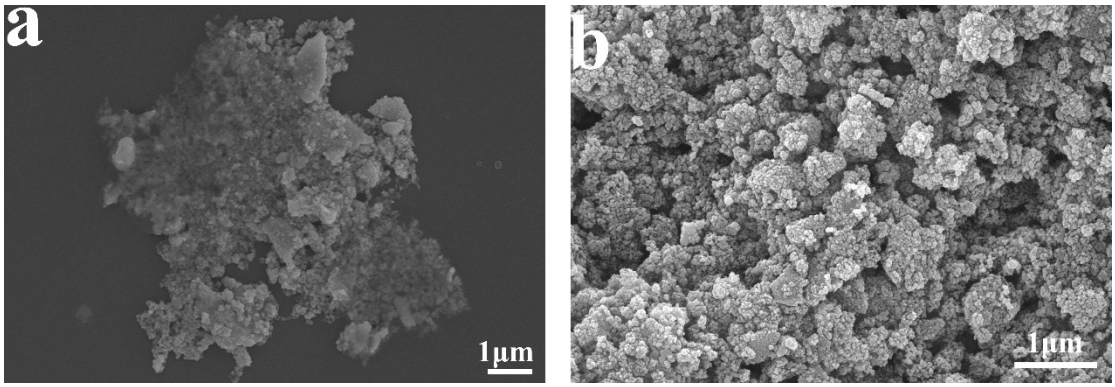

Fig. S4 The SEM images of (a) TaON@Gr and (b) TaO/TaN@Gr.

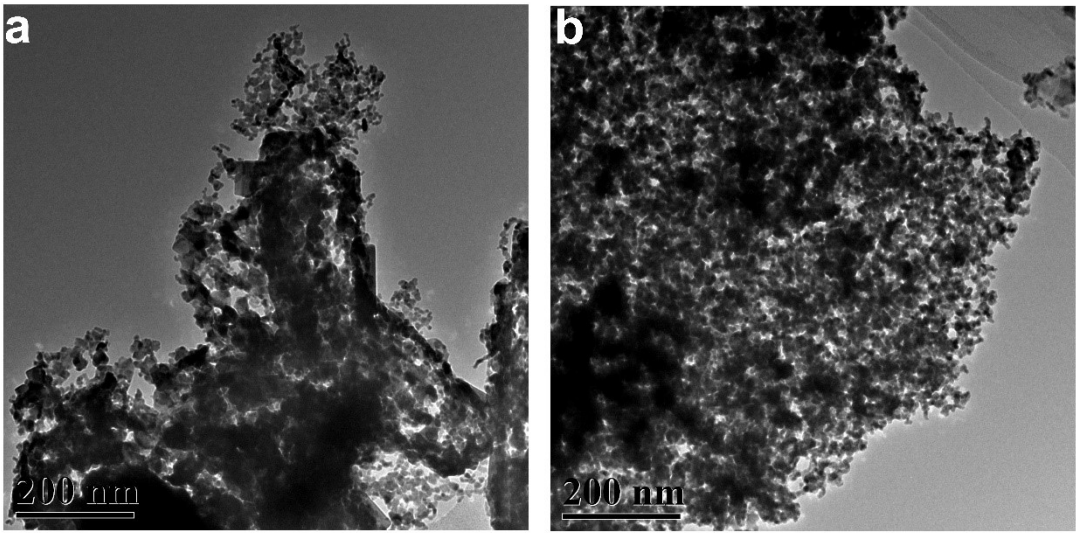

Fig. S5 The TEM images of (a) TaON@Gr and (b) TaO/TaN@Gr.

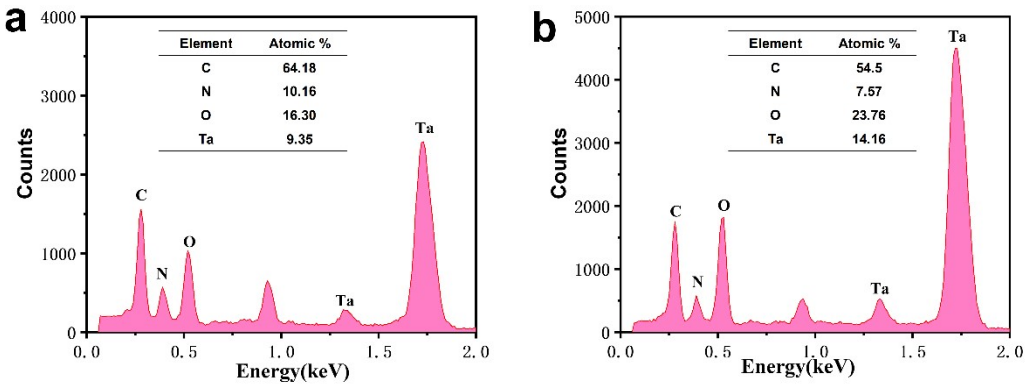

Fig. S6 TEM-EDS patterns of (a) TaON@Gr and (b) TaO/TaN@Gr catalyst.

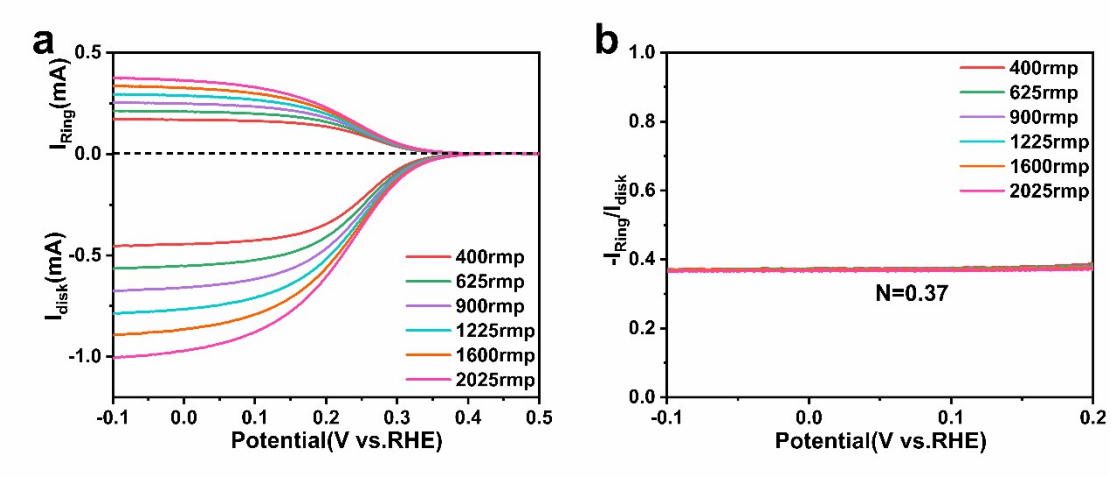

Fig. S7 (a) The LSV curves in 1 M KCl+10 mM $K_3[Fe(CN)_6]$ at different rotate speeds, (b) the collection efficiency (N) for RRDE.

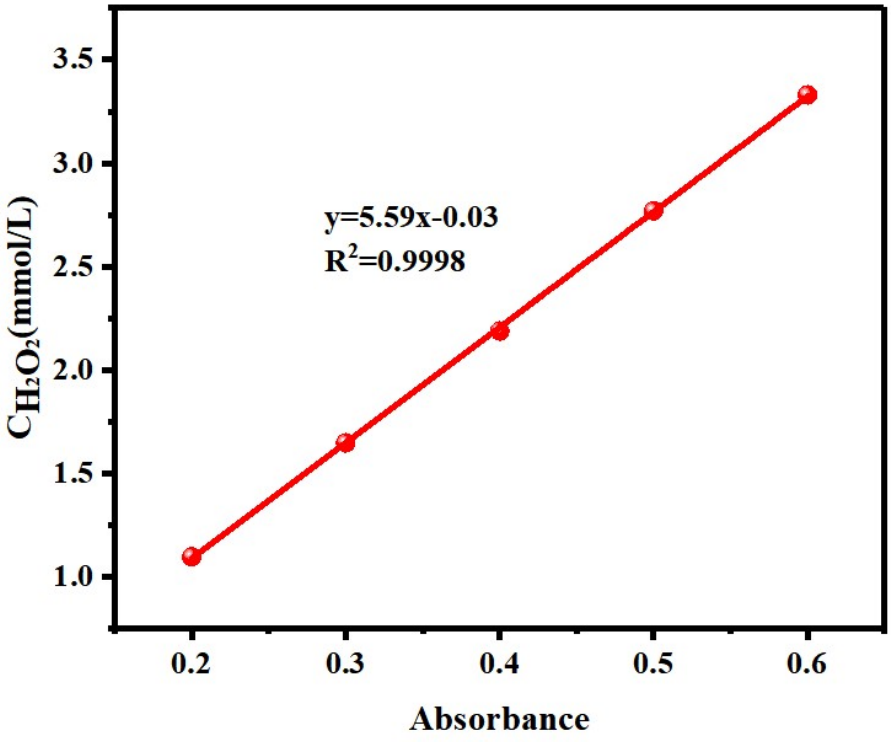

Fig. S8 H_2O_2 concentration-absorbance standard curve.

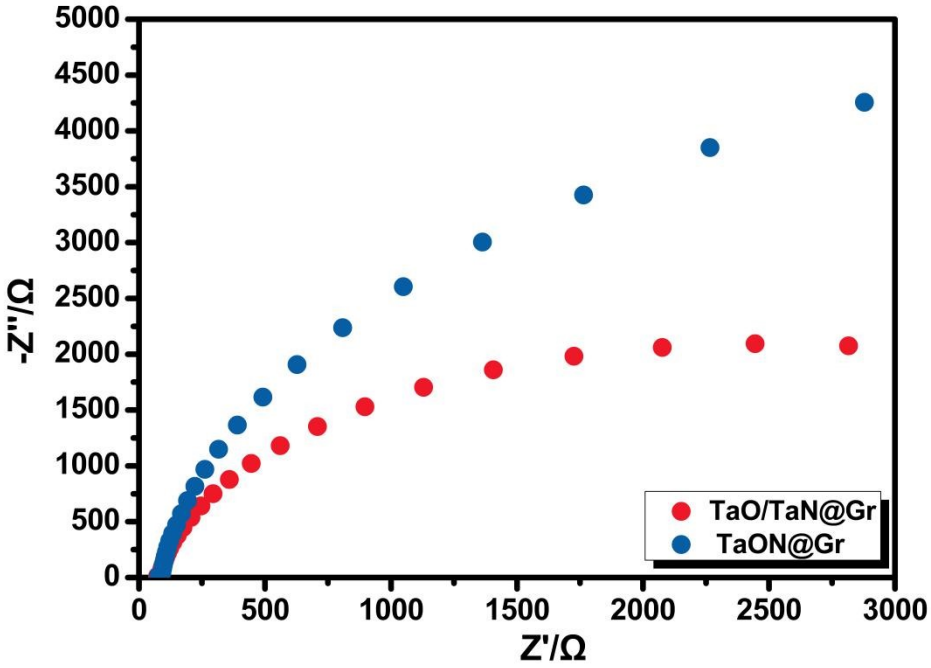

Fig. S9 The EIS curves of TaON@Gr and TaO/TaN@Gr.

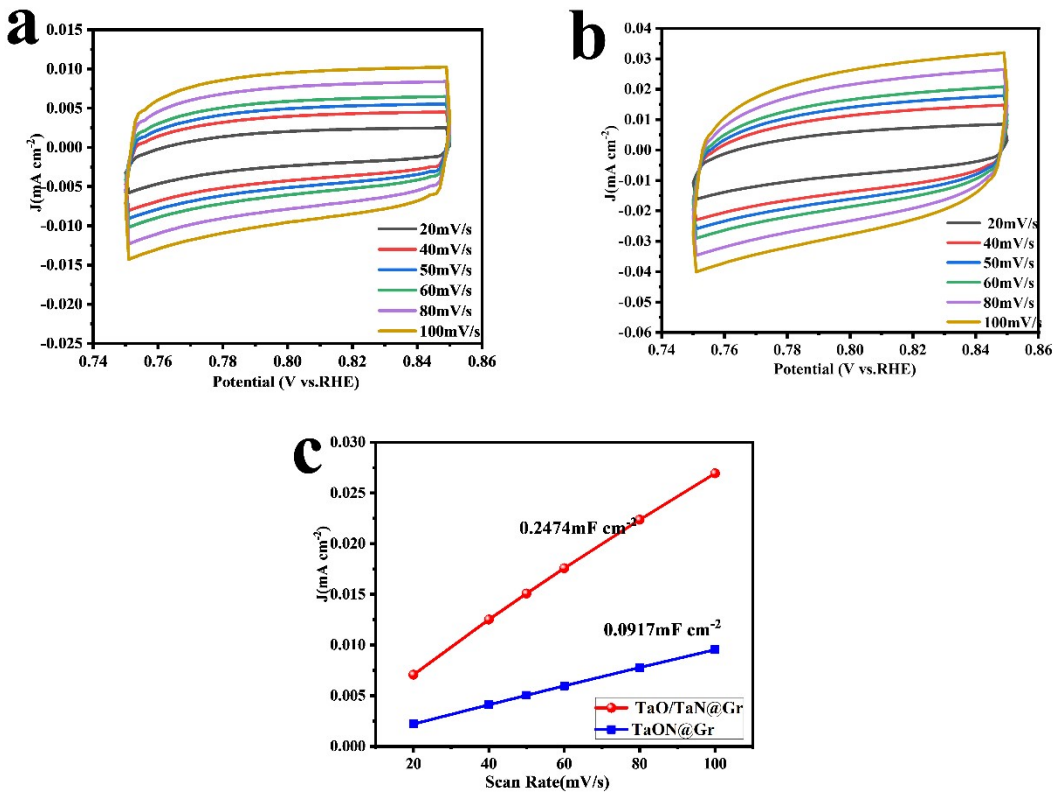

Fig. S10 CV curves of (a) TaON@Gr and (b) TaO/TaN@Gr in the region of 0.75~0.85 V_{RHE} with various scan rates for 2e- ORR, and (c) their corresponding C_{dl} curves.

$$ECSA_{TaO/TaN@Gr} = \frac{0.247\ mF\ cm^{-2}}{40\ \mu F\ cm^{-2}\ per\ cm^{2}_{ECSA}} = 6.175\ cm^{2}_{ECSA}$$

$$ECSA_{TaON@Gr} = \frac{0.0917\ mF\ cm^{-2}}{40\ \mu F\ cm^{-2}\ per\ cm^{2}_{ECSA}} = 2.2925\ cm^{2}_{ECSA}$$

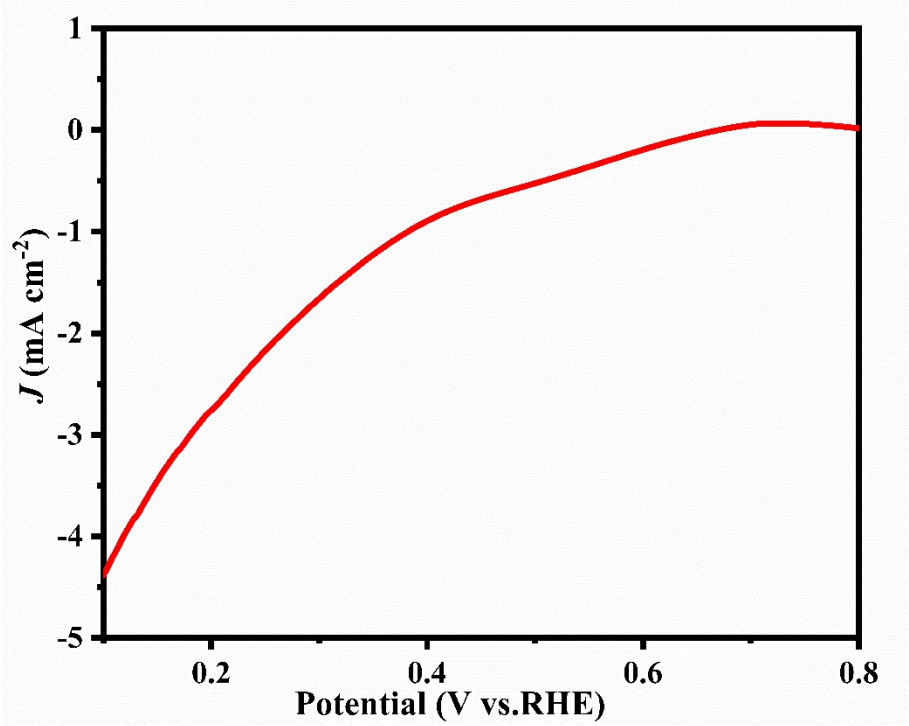

Fig. S11 The ORR polarization curve of TaO/TaN@Gr in the H-type cell configuration.

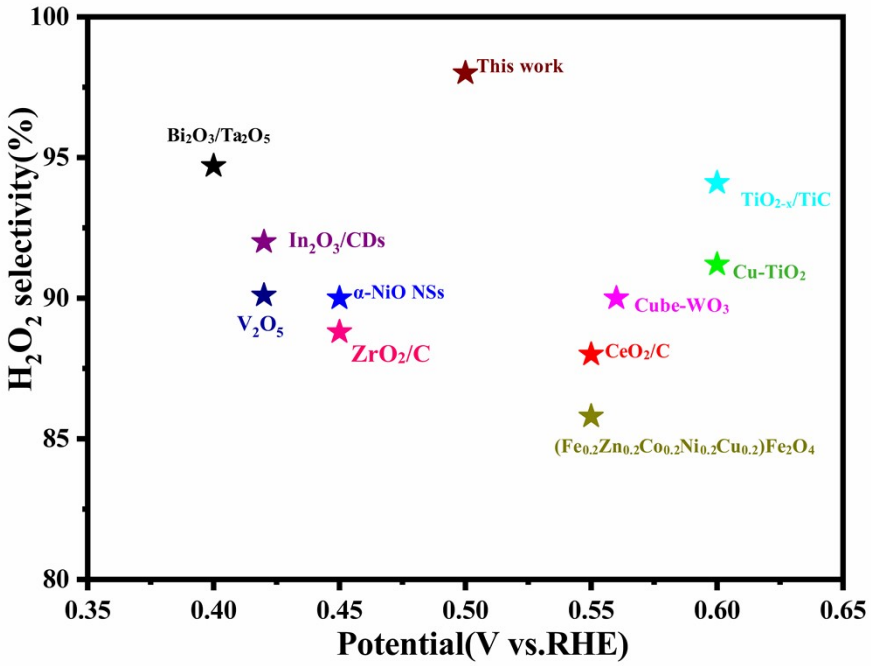

Fig. S12 The comparison of $2e^-$ ORR selectivity for TaO/TaN@Gr and recently reported electrocatalysts.